JOURNAL OF AIRCRAFT
Vol. 48, No. 3, May–June 2011

Numerical Optimization and Experimental Investigations on the Principle of the Vortex Diffuser

Stefan Puttinger,* Andreas Mehrle,† and Philipp Gittler‡
Johannes Kepler University of Linz, 4040 Linz, Austria
and
Walter Meile§
Graz University of Technology, 8010 Graz, Austria

DOI: 10.2514/1.C031013

The present work deals with numerical optimization of and experimental studies on aftmounted wingtip devices, or so-called vortex diffusers. The purpose of most kinds of wingtip devices is to reduce the induced drag by converting vortex energy into thrust. To obtain an optimal design for the vortex diffuser, the parameterized diffuser blade shape is optimized with respect to axial thrust within the framework of the lifting-line theory. Finite airfoil performance is accounted for by applying lift and drag coefficients from wind-tunnel data. The so-gained optimal design for the vortex diffuser blades is realized on a small-scale model, and wind-tunnel tests are carried out to investigate drag reduction of the vortex diffuser for comparison with numerical results. Furthermore, the goal is to gain some experience and data for preparation of real flight testing on an unmanned aerial vehicle. As the vortex diffuser can produce forces and moments in all three directions, a pure wing–body configuration with vortex diffusers instead of rudder, elevator, and ailerons would be possible. The wind-tunnel tests also deliver data to investigate basic flight mechanics of such a configuration. In the case of asymmetric vortex roll up, the paper demonstrates a way to optimize the vortex diffuser settings online in the wind tunnel. Experiments clearly show that the vortex diffuser is able to reduce drag in high-lift/high-angle-of-attack configurations. Wind-tunnel tests, however, also demonstrate some problems for practical design of the vortex diffuser.

Nomenclature

b	=	span, m
C_D	=	drag coefficient
C_L	=	lift coefficient
C_M	=	pitching-moment coefficient
C_R	=	rolling-moment coefficient
C_S	=	side-force coefficient
C_Y	=	yawing-moment coefficient
D_{VD}	=	drag force at vortex diffuser, N
L_{VD}	=	lift force at vortex diffuser, N
M_M	=	pitch moment, Nm
M_R	=	roll moment, Nm
M_{VD}	=	moment of vortex diffuser, Nm
M_Y	=	yaw moment, Nm
n	=	number of vortex diffuser blades
r	=	radial coordinate outside the body of revolution, m
R_c	=	radius of body of revolution, m
R_d	=	radial extent of vortex diffuser, m
S_{VD}	=	side force at vortex diffuser, N
u_∞	=	freestream velocity, m/s
w	=	tangential velocity, m/s
$\mathbf{x}$	=	argument vector of object function
x_{VD}	=	x coordinate of vortex diffuser center, m
y_{VD}	=	y coordinate of vortex diffuser center, m
z_{VD}	=	z coordinate of vortex diffuser center, m
α_g	=	geometric angle of attack, °
α_{VD}	=	local angle of attack of vortex diffuser blades, ° (with reference to calculated optimal angle of attack)
$\bar{\alpha}_{\mathrm{VD}_i}$	=	nondimensional blade angles
Γ	=	circulation of vortex diffuser blade, m^2/s
Γ_0	=	circulation of main wing, m^2/s
Λ	=	aspect ratio

Presented as Paper 2009-3610 at the 27th AIAA Applied Aerodynamics Conference, San Antonio, TX, 22–25 June 2009; received 9 March 2010; revision received 21 December 2010; accepted for publication 4 January 2011. Copyright © 2011 by the American Institute of Aeronautics and Astronautics, Inc. All rights reserved. Copies of this paper may be made for personal or internal use, on condition that the copier pay the $10.00 per-copy fee to the Copyright Clearance Center, Inc., 222 Rosewood Drive, Danvers, MA 01923; include the code 0021-8669/11 and $10.00 in correspondence with the CCC.

*Senior Scientist, Institute of Fluid Mechanics and Heat Transfer; stefan.puttinger@jku.at.
†Senior Scientist, Institute of Fluid Mechanics and Heat Transfer; andreas.mehrle@mci.edu.
‡Head of Department, Institute of Fluid Mechanics and Heat Transfer; philipp.gittler@jku.at.
§Assistant Professor, Institute of Fluid Mechanics and Heat Transfer; meile@fluidmech.tu-graz.ac.at.

I. Introduction

INDUCED drag due to the vorticity released from the wingtips of an aircraft is a major part of the total drag in cruise flight and increases further in other flight phases. Various approaches exist to reduce the vorticity and, hence, the induced drag of an airplane; see Kroo [1] for a review on principles and devices. Most classical approaches, besides increasing span, make use of an extended or closed wingtip design (winglet, wing grid, C wing, and spiroid wing). On the contrary, a so-called vortex diffuser, which was first proposed by Hackett [2], is situated behind the trailing edge at the wingtip. While conventional designs, like winglets, try to reduce the wingtip vortex in strength, the goal of aftmounted devices like the vortex diffuser is to regain some of the energy contained in the vortices. The idea behind it is that, by increasing (diffusing) the core radius of the vortex, the contained kinetic energy, and thus the induced drag, is reduced. Figure 1a illustrates the change in crossflow velocity w for a Rankine vortex if the constant circulation Γ_0 is displaced to a bigger radius. Figure 1b shows the principal design of a vortex diffuser. The number of blades n is basically arbitrary, but since skin friction increases with n, a blade number of four turns out to be a good compromise (see Sec. II).

While Hackett [2] experimented with the number and positioning of the vortex diffuser blades, no effort was taken to optimize the shape of the blades to gain a maximum of thrust. In the present paper, the authors outline a systematic approach to the vortex diffuser concept. As the vortex roll-up mechanism is very complex and strongly dependent on wing section and wing planform, this work

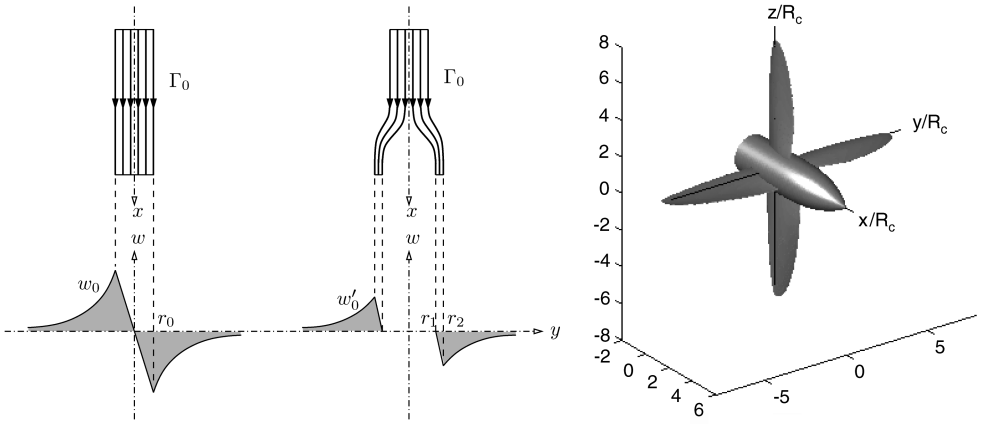

a) Rankine vortex (left) and diffused Rankine vortex (right) **b) Arrangement of four vortex diffuser blades on body of revolution**

Fig. 1 Principle of vortex diffuser.

does not intend to give general guidelines for a vortex diffuser design. Rather, it should be seen as a detailed proof-of-concept study showing possible ways for designing and optimizing a complex wingtip device like a vortex diffuser.

To produce a strong wingtip vortex, a rectangular planform with a high-lift wing section (SD7062; Fig. 2a) is chosen as the basis for further discussion. Wimmer [3] investigated the vortex roll up of such a wing in detail by use of particle image velocimetry (PIV). His results clearly show that, for high angles of attack, shortly behind the wing, the shed circulation is absorbed in the trailing vortex to a very high degree, producing a nearly axisymmetric wingtip vortex. The PIV analysis of the vortex roll up led to the inclination angles of the axes of the body of revolution for a high-angle-of-attack configuration, seen in Fig. 3a [3].

After analyzing the wingtip vortex, a numerical calculation of the optimal shape for the vortex diffuser blades was done. As this obviously leads to an iterative optimization problem, a fast algorithm is necessary to get results within an acceptable computing time. Therefore, a Navier–Stokes-based calculation is not a practical approach. The method described in the next section is based on an extension of the lifting-line theory for an axisymmetric geometry like the vortex diffuser and is able to deliver an optimal blade design very quickly. Based on the PIV measurements of Wimmer [3], an axisymmetric flow situation is assumed as an input boundary condition for the blade shape calculations. In this case, only a thrust in the x direction and a roll moment around the same axis act on the diffuser. This moment slightly increases the root bending moment of the wing. However, the increase of bending moment by increase of span is much higher than the increase of moment due to the vortex diffuser (based on the same percentage of drag reduction).

The so-achieved vortex diffuser design was then adopted for a wind-tunnel model and investigated mainly in high-angle-of-attack configurations.

II. Numerical Approach

Because of the highly three-dimensional flow situation behind the wingtips, an accurate wing design is crucial in order to obtain a net thrust from the vortex diffuser. A calculation method is needed that is fast enough to serve as an object function in an optimization procedure but, at the same time, is sufficiently accurate to reliably calculate thrust and moment of the vortex diffuser assembly. Once the calculation method is found, the shape of the vortex diffuser blades may be parameterized, and the optimal shape may be found in an iterative process.

For the design phase of the process, Navier–Stokes-based solvers are not adequate due to the excessive meshing and solving effort; cf., Krieger [4], who evaluated a configuration considered optimal with a commercial finite volume code. Furthermore, especially when calculating drag, full Navier–Stokes still fall short of the necessary accuracy when compared with experimental results. A panel method in combination with drag evaluation in the Trefftz plane seems to be a good candidate. Unfortunately, the interaction of the trailing vortices leads to spurious results and prohibits the use of an optimizer. The calculation of viscous drag components is possible, but it is neither adapted to three-dimensional flow situations nor sufficiently accurate. Although considered outdated, lifting-line theory may calculate dozens of solutions within a few seconds, which makes it a perfect calculation tool for an iterative optimization process. With the incorporation and interpolation of airfoil performance data obtained from wind-tunnel measurements, the fidelity of the drag calculation is as high as the quality of the empirical data used. Still, several shortcomings need to be overcome. They consist of the following:

1) The onflowing vortex shape cannot be calculated with the lifting-line method.

2) The lifting line is not adapted to axisymmetric flow situations.

3) The actual airfoil shape corresponding to the circulation distribution has to be calculated.

Such a method is described by Mehrle [5]. Starting from a series representation of the circulation Γ along the radial coordinate, the induced downwind and thrust from Kutta–Joukowsky's law can be found for a periodic lifting system like the vortex diffuser. Making use of tabulated airfoil data, the profile drag is calculated. Since operating the airfoil at optimal gliding ratio is an auxiliary condition for thrust maximization, the wing shape (chord length and angle of attack) is uniquely determined by the circulation distribution.

A modification is only needed in what concerns the inner extremity of the wings. Since the vortex diffuser wings are mounted on a body of revolution, the circulation imposed on the wing has to be mapped inside the body according to

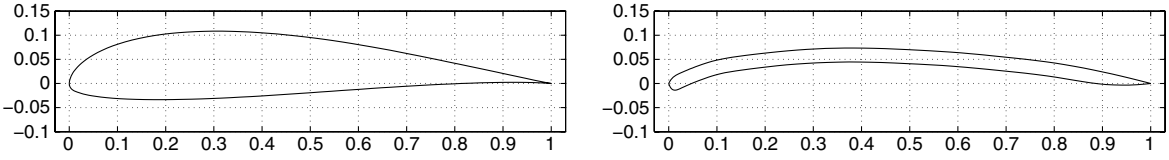

a) SD7062 **b) Goe417a**

Fig. 2 Contours of used wing and blade section profiles.

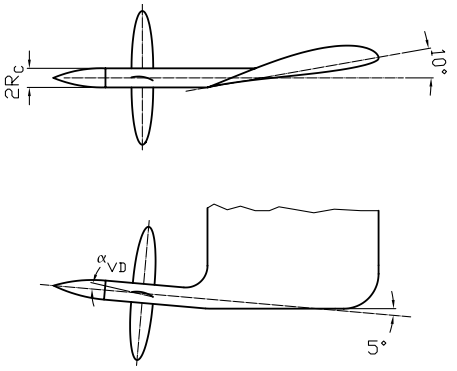

a) Inclination of axis of body of revolution for high angle of attack

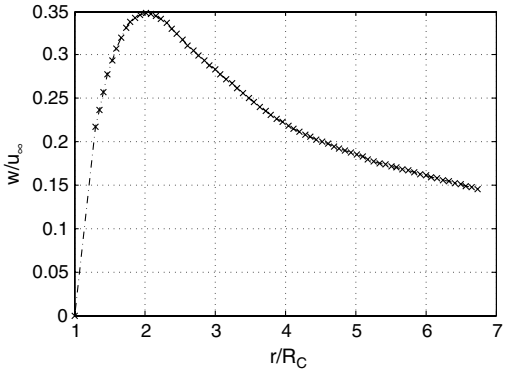

b) Nondimensional tangential velocity w/u_∞ over nondimensional radius r/R_c (data taken from PIV measurements of Wimmer [3])

Fig. 3 Geometry and tangential velocity.

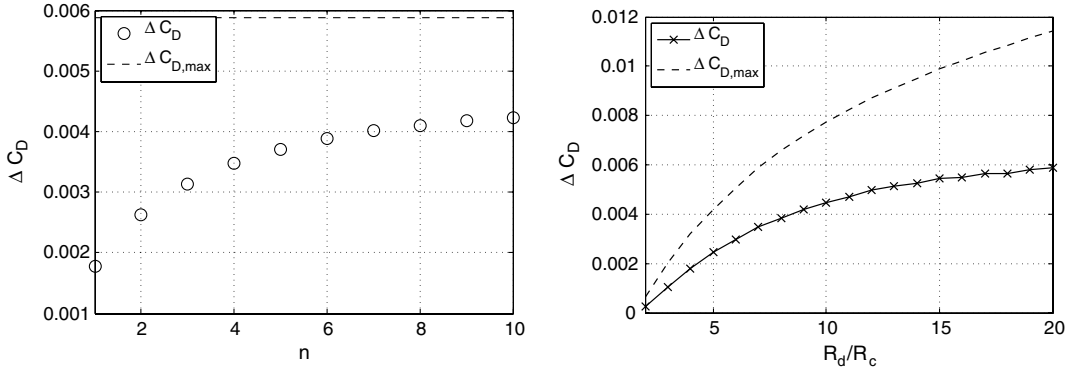

a) b)

Fig. 4 Vortex diffuser performance as function of a) number of blades n and b) radial extent R_d of the vortex diffuser.

$$\Gamma(r) = \Gamma(R_c^2/r) \quad \text{for } r < R_c \tag{1}$$

However, only the circulation around the wing contributes to the thrust generation. Minimal drag is found by optimizing Γ with a quasi-Newton method with a cubic line search procedure with respect to maximal vortex diffuser thrust.

Parameters influencing vortex diffuser performance, other than the number of blades n (see Fig. 4a), are the radial extent R_d and the airfoil performance. The latter could be shown to be insignificant. While in an inviscid case, the kinetic energy of the vortex is fully converted into thrust for drag minimization; accounting for viscosity, a residual of the circumferential velocity component $w = u_\infty/\varepsilon$ yields the optimal thrust. If u_∞ and the vortex velocity w_0 are of the same order of magnitude, which is typically the case near the body of revolution, the actual value of ε plays only a secondary role; cf., [5,6] for details. For spans larger than $8 \cdot R_c$, configuration disadvantages outweigh performance gains; see Fig. 4b. The dashed line represents a theoretical limit due to the conservation of energy (inviscid optimum):

$$F_x u_\infty < \frac{\rho u_\infty}{2} \int_A w^2 \, \mathrm{d}A' = \pi \rho u_\infty \int_{R_c}^{R_d} r w^2 \, \mathrm{d}r \tag{2}$$

In this study, the radial extent was chosen to be $R_d = 7 \cdot R_c$.

Taking the vortex as measured by Wimmer [3] for an angle of attack of 10° as the onflow condition (see Fig. 3b) and the characteristics of the Goe417a airfoil as measured by Schmitz [7] (see Fig. 5¶), the optimization procedure predicts a thrust generation of $\Delta C_D = -0.0035$ ($\approx$10% of the total drag for two diffusers) for each vortex diffuser. The corresponding wing chord and twist are given in Fig. 6. For Reynolds numbers typically encountered at full-size aircraft, the drag reduction is as high as $\Delta C_D = 0.0044$.

¶The term (1) used in some figures denotes nondimensional values.

III. Wind-Tunnel Tests

A. Measurement Techniques

For wind-tunnel testing, a model-scale vortex diffuser was built according to Fig. 3a. The position of the vortex diffuser was $x_{\mathrm{VD}}/b = 0.232$ behind the trailing edge.

The main wing has a rectangular planform with a chord length of 250 mm and an aspect ratio of six. To produce a strong wingtip vortex to put the vortex diffuser in, we need a profile that is applicable for high-lift/high-angle-of-attack configurations. Among other candidates, we found the Selig-Donovan SD7062 (Fig. 2a) best suited for our needs. Other candidates would be the Wortman FX63-137 or Selig S1223. As the same profile will be used for the wings of an experimental unmanned aerial vehicle (UAV), we preferred the easier to fabricate SD7062, which is probably also more robust in use (compared with the very small trailing edge with high camber of the FX63-137). Two different wing models were used in the wind-tunnel tests, as will be described later.

All tests were done in the low-speed wind tunnel of the Institute of Fluid Mechanics and Heat Transfer at Graz University of Technology. The wind tunnel has a cross section of 2×1.46 m and a longitudinal turbulence level of 0.13%.

Since this is a general purpose wind tunnel, neither flow quality nor force balance accuracy are comparable with wind tunnels specially designed for low-speed aerodynamic investigations. So agreement in lift and drag forces with data from other test facilities might not be satisfactory, but this was not the primary goal of our study. In fact, a different approach was taken to investigate the differences in drag due to the use of a vortex diffuser.

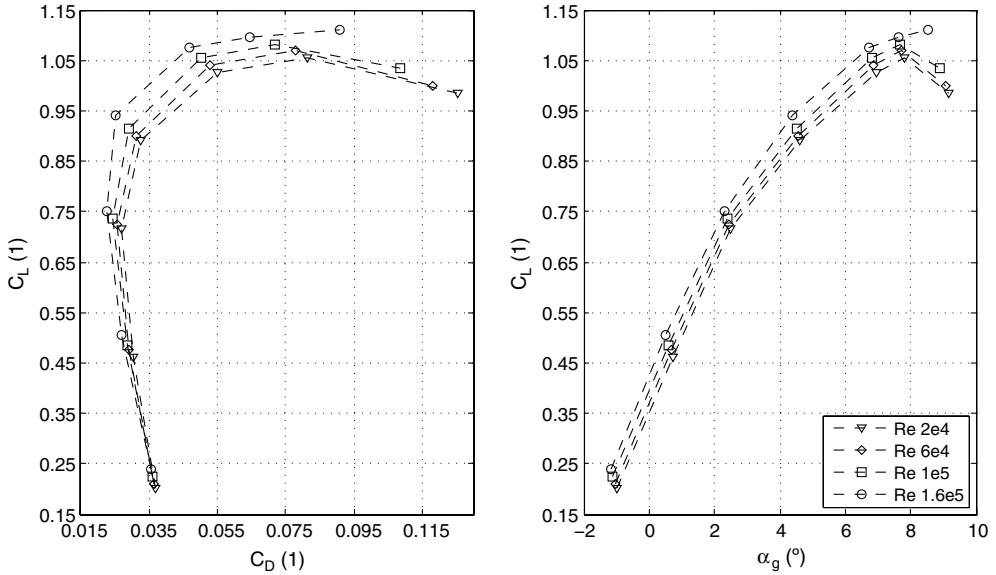

Fig. 5 Lift and drag data for Goe417a as documented by Schmitz [7].

Three series of wind-tunnel tests have been carried out. In the first series, only drag was measured by replacing the standard six-component platform balance with a specially designed balance, with a high-sensitivity load cell covering a force range of 0.3 N, with a total error of 0.0067% of rated output. The wing was mounted on a slide moving on linear bearings pushing onto the load cell (Fig. 7a). In this series, the focus was to resolve the relative differences in drag without and with the vortex diffuser.

In the second and third series, full data were recorded with the six-component platform balance, which turned out to have adequate resolution for airfoil measurements when used with an appropriate amplifier. Accuracy of all forces and moments on the platform balance was found to be better than 0.5%.

While the second series was used to investigate the influence of the vortex diffuser on lift and moments, the third series was focused on the problem of asymmetry in the vortex roll up. Complete documentation of all conducted wind-tunnel tests can be found in [8].

The angles of attack measured were 0, 5, and 10° for the first series and 0, 4, and 10° for the second and third series. The accuracy of angle adjustment is about 0.1°.

Tests have been carried out at Reynolds numbers of 160,000 and 600,000. For the vortex diffuser blades, the velocities correspond to Reynolds numbers of 30,000 and 120,000, respectively. Expected drag forces for the SD7062 according to data from Lyon et al. [9] and Selig et al. [10] are around $C_D = 0.079$ if converted for an aspect ratio of six.

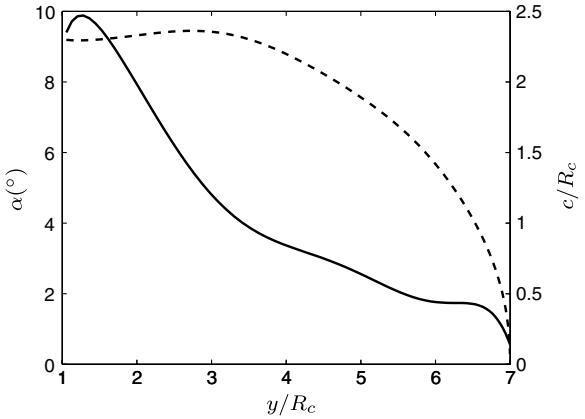

Fig. 6 Calculated twist (solid line) and chord length (dashed line) of vortex diffuser blades.

For the experiments with the drag balance, the original wing built by Wimmer [3] was used. This model was made of a computer numerically controlled cut foam core covered with epoxy–glass resin and then painted and polished. As it was not possible to mount that wing on the platform balance, a second model was built with the same core, but it was planked with balsa wood, polished, and covered with foil. This wing has therefore a smoother surface than the painted one. This might be one of the reasons for the differences in the wind-tunnel results and the formation of the wingtip vortex discussed later, since aerodynamic behavior is very sensitive to surface quality in the range of the lower Reynolds number under test.

B. Results

Experiments with the drag balance showed good agreement with expected forces. Figure 8a clearly demonstrates that the vortex diffuser is able to reduce drag by about 16% for high angles of attack. Agreement with predicted drag reduction is very good.

For medium and low angles of attack, however, there is always an increase in drag. Drag forces for a 0° angle of attack are close to the threshold of the balance, so that the results exhibit a high level of uncertainty.

To check for optimal settings of the vortex diffuser blades, the angle of the blades has been varied in steps of ±2°, based on their calculated optimal position relative to the axis of the body of revolution. Figure 8b shows that the prediction of optimum settings for the vortex diffuser blades for $\alpha_g = 10°$ for the main wing is correct. Even for $\alpha_g = 0°$, the calculated position seems to produce minimal drag, although the local flow direction on the vortex diffuser blades changes significantly. For $\alpha_g = 5°$, there is no clear picture. Increasing, as well as decreasing, the local angle of attack seems to reduce drag. Further experiments have to be done here. To minimize the increase of drag due to the vortex diffuser at low angles of attack, not only the local angle of attack of the vortex diffuser blades but also the incidence angle of the vortex diffuser axis should be reduced. A variable inclination angle for the body of revolution axis where the vortex diffuser blades are mounted is foreseen for the next version of the vortex diffuser model.

Figure 9 shows the relative change for all forces and moments due to the vortex diffuser and the body of revolution compared with the rounded wingtip. All data were gained in the second wind-tunnel series by use of the six-component platform balance. Data labeled with *Re 6e5* were taken at a high Reynolds number, and all other data were taken at a Reynolds number of 160,000, as before. The identifier BOR is assigned to data taken only with the body of revolution without vortex diffuser blades.

a) Drag balance b) Vortex diffuser model c) Body of revolution

Fig. 7 Setup of wind-tunnel experiments.

Side forces vary notably between the configurations (Fig. 9e), but as absolute side forces are very low (lower than drag forces), these variations are overestimated in the relative scale. Moment data in Fig. 9 confirm the expected behavior. Pitch moment C_M is reduced by the vortex diffuser. Yaw moment C_Y correlates with the increase or decrease in drag and roll moment C_R with the lift variation.

Measured lift forces were much lower than expected. The reason for this was partially found in a flow separation on the wing close to the tunnel floor caused by a horseshoe vortex. Therefore, a boundary-layer suction on the low-pressure side of the wing was applied in some measurements at the lower Reynolds number to improve the overall flow situation on the main wing. As the boundary-layer suction yields only a small improvement in lift data, the decrease in lift due to the vortex diffuser must have multiple reasons. Drag improvement is also quite poor in comparison with the measurements with the drag balance. Flow visualization with filaments led to the suspicion that the second wing with foil cover shows a different vortex roll-up behavior in the wind tunnel. This will therefore not lead to the axisymmetric flowfield seen in the PIV experiments and presumed in the numerical computation. As a conclusion, we have to assume for our wind-tunnel model that every vortex diffuser blade experiences a different local flow condition, thus producing different forces. Therefore, the vortex diffuser is not force free in the y-z plane and produces unwanted forces superposing lift and side forces.

A detailed analysis of the wind-tunnel results shows that, if we apply the difference measured in C_L, C_D, and C_S between the test configuration with the vortex diffuser and the configuration with the body of revolution at the center point of the vortex diffuser (Fig. 10a), and we calculate the resulting moments in the point of origin at the quarter-line of the main wing (equal to the mounting point of the wing on the platform balance), we get good agreement with the real measured moment differences ΔM_M, ΔM_R, and ΔM_Y in this point between these two configurations (Fig. 10b). These results clearly identify that the vortex diffuser does not experience a symmetric flow condition on our wind-tunnel model and, hence, produces unintended lift and side forces as long as the same local angle of attack is used for all blades. These forces acting on the vortex diffuser explain the reduction of lift seen in Fig. 9a. The correct reference for this comparison has to be the body of revolution instead of the rounded wingtip, since the body of revolution without vortex diffuser blades already reduces lift by about 2% (Fig. 9a).

Now, if total lift is reduced, one could argue that induced drag should decrease equivalently. However, the reduction of total lift results mainly from the downforce generated at the vortex diffuser, not from a decrease of the lift of the main wing. However, induced drag due to the lift of the main wing can be considered constant. In fact, the total induced drag rises, since the vortex diffuser represents another lift producing area, hence generating additional induced drag proportional to the lift and side forces mentioned previously and seen in Fig. 9. This additional drag compensates some of the gained thrust and explains the bad drag performance found in the second measurement series (overall drag reduction between 2 and 6%). This also explains part of the discrepancies in the absolute numbers of measured drag forces with $C_D = 0.066$ and $C_D = 0.088$ ($Re=$ $1.6e5$ and $\alpha_g = 10°$) between the two wings.

C. Rudder Forces and Moments

The vortex diffuser is able to generate all forces and moments needed to control and navigate an aircraft. So, if the upper and lower vortex diffuser blades are rotated simultaneously in the same direction, one can generate a yaw moment (rudder function). If the inner and outer blades are rotated simultaneously, a pitch and/or roll moment results (aileron/elevator function). Therefore, a flying wing design with vortex diffusers as the main steering device seems possible. Such a configuration would have the big advantage of reducing overall drag by removing the tail with rudder and elevator and could therefore compensate the drag increase due to the vortex diffuser (mainly due to increased skin friction) for low angles of attack. Figure 11 shows the CAD model of a modular UAV in two possible outlines. The plane was built for student projects and is already flying in conventional configuration without a vortex diffuser

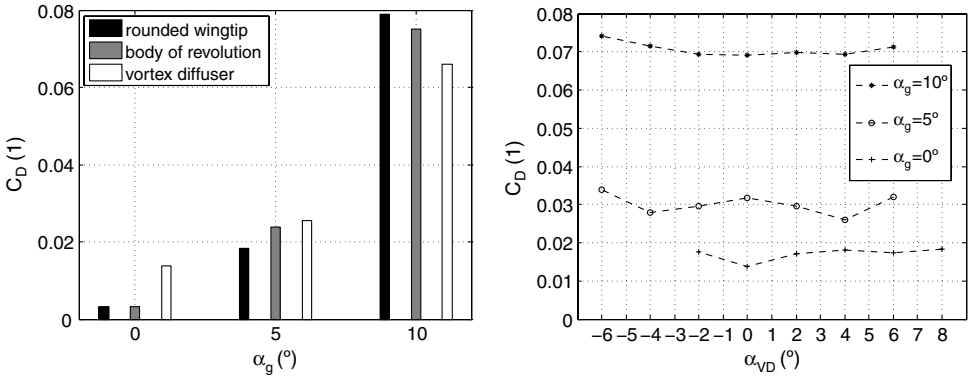

a) b)

Fig. 8 Drag data from first series for a) different angles of attack and b) variation of vortex diffuser blade angle with reference to calculated optimal angle of attack.

to collect flight mechanics data for further analysis. In the CAD figure, the orientation of the vortex diffuser blades is rotated by 45° in reference to the trailing edge. This angle is basically arbitrary. But as a first step for the understanding of flight mechanics, it is easier to keep the inner blade aligned with the trailing edge. This was also the configuration used in the wind-tunnel tests (see Fig. 7b).

As a starting point to analyze the flight mechanics of a vortex diffuser, the blade pairs were rotated in steps of 10° in the range of ±30° from their calculated neutral positions. Figure 12 illustrates all six forces and moments generated relative to the respective value for the neutral position.

Correlations of forces and moments are as expected. If lift is increased by increasing the local angle of attack, the negative pitch and roll moments increase in the same manner. Any change in blade angle leads to an increase in drag and an increase in yaw moment, respectively. As is desirable, the strongest coupling exists between side force and yaw moment. The roll moment has a slight negative coupling with the yaw moment, which means that lift slightly increases on the right side if a right turn is intended. Such a behavior can also be noticed in other flying systems mainly controlled by increasing drag, like paragliders. If deflections of blade angles are limited to a range of ±10°, a linearized model to describe steering with a vortex diffuser could be used.

D. Online Optimization in Wind Tunnel

To account for asymmetry of the vortex roll-up process on our wind-tunnel model, a third measurement series was conducted with online optimization of the individual vortex diffuser blade settings to gain optimal drag reduction. Figure 13a shows the optimization loop, which is based on the mathematical formulation for a constrained minimum search:

$$\min_{\mathbf{x}} C_D(\mathbf{x}) \qquad \mathbf{x}_{\min} < \mathbf{x} < \mathbf{x}_{\max}$$

As we want a nondimensional formulation for the optimization process, we define the nondimensional blade angles as follows:

$$\bar{\alpha}_{\mathrm{VD}_i} = \frac{\alpha_{\mathrm{VD}_i} - \alpha_{\mathrm{VD}_{i,\min}}}{\alpha_{\mathrm{VD}_{i,\max}} - \alpha_{\mathrm{VD}_{i,\min}}}$$

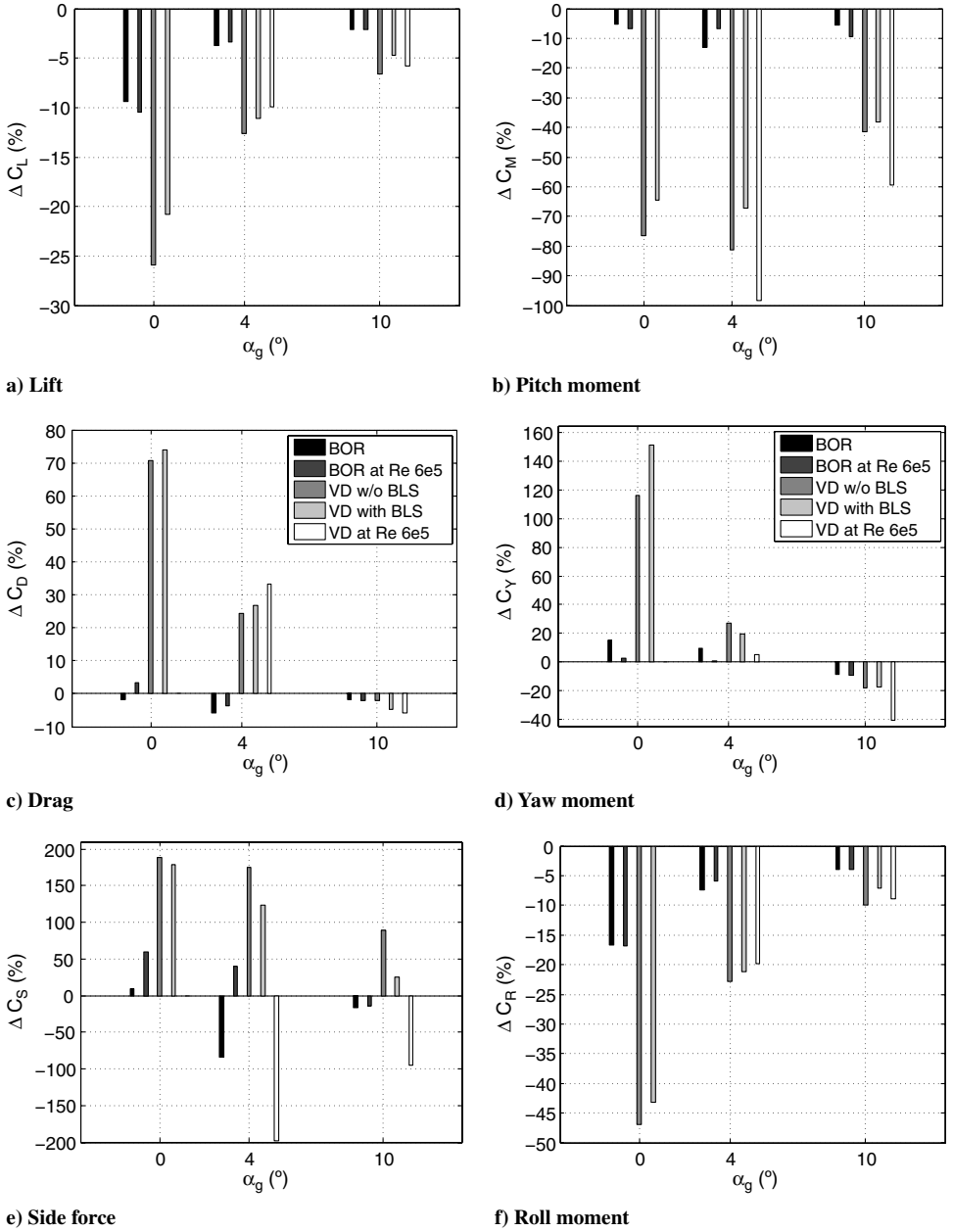

a) Lift **b) Pitch moment**

c) Drag **d) Yaw moment**

e) Side force **f) Roll moment**

Fig. 9 Forces and moments for vortex diffuser (VD) with and without boundary-layer suction (BLS) and body of revolution (BOR).

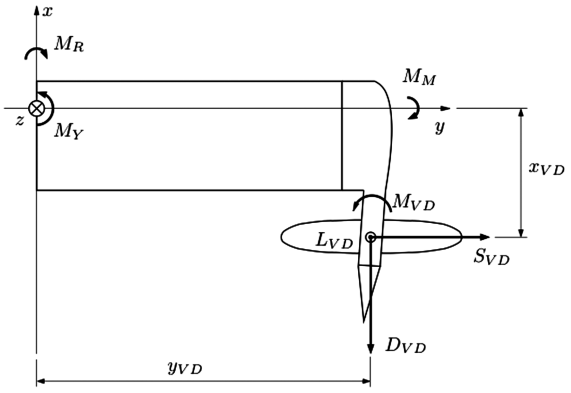

a) Forces acting on vortex diffuser for nonaxisymmetric flow condition

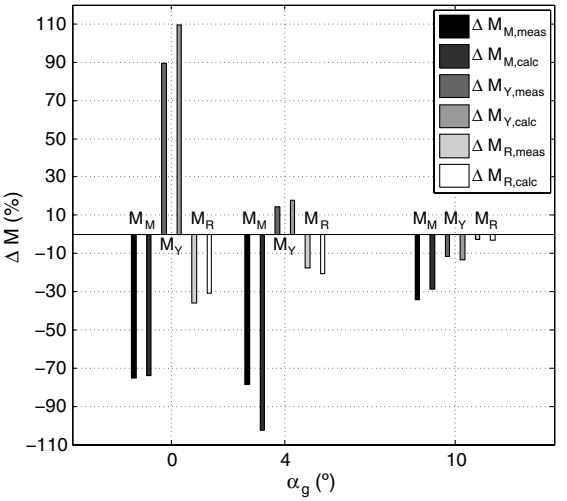

b) Comparison of measured and calculated moment data from vortex diffuser and body of revolution

Fig. 10 Forces and moments on vortex diffuser due to asymmetry.

and form the vector $\mathbf{x}$ of nondimensional blade angles to be used as the argument for the object function:

$$\mathbf{x} = [\bar{\alpha}_{\mathrm{VD}_1}, \bar{\alpha}_{\mathrm{VD}_2}, \bar{\alpha}_{\mathrm{VD}_3}, \bar{\alpha}_{\mathrm{VD}_4}]$$

The algorithm and data processing was implemented in MATLAB using the data acquisition and optimization toolboxes.

As the load cells of the platform balance need some time to give the correct values for a new setting, a settling time of 15 s was inserted. The measuring time was also 15 s. To visualize the optimization progress, a norm of the blade angle vector is formed by

$$\|\mathbf{x}\| = \sqrt{\bar{\alpha}^2_{\mathrm{VD}_1} + \bar{\alpha}^2_{\mathrm{VD}_2} + \bar{\alpha}^2_{\mathrm{VD}_3} + \bar{\alpha}^2_{\mathrm{VD}_4}} \tag{3}$$

Drag data are plotted over $\|\mathbf{x}\|$, which is scaled to the maximum possible norm of blade angles. In addition, data points (Fig. 13b) are shaded from light gray (starting point x_s) to black (final value x_f). Figure 13b shows a typical optimization run starting at blade angles well out of the calculated zero position and approaching a minimum drag at low angle deflections in the lower left part of the plot. For start values close to the zero position, the optimization would start from a region in the upper left corner, going down to the lower left corner as before.

Optimization results show the expected behavior and deliver asymmetric blade angles for most cases. Thus, the authors could demonstrate that an online optimization in a wind tunnel is possible and delivers repeatable results. However, several difficulties occur because of the fact that we have a real life experiment instead of an analytical formulation to be used as an object function in the optimization process. The following points are limiting the quality of the optimization, either due to the limitations of the available equipment or the physical flow behavior:

1) As a result of very small differences in the drag force for small changes in the blade angles, the optimization process is limited by the experimental setup (load cells, amplifier, etc.). In other words, the signal-to-noise ratio decreases for small changes in the blade angles. If x_s is badly chosen in such a case, the optimization process tends to get stuck in a local minimum instead of finding a global minimum. Figure 14 shows that while, for a start value of $\mathbf{x}_s = [5, 5, 5, 5]$ a reproducible result is found, there is no optimization possible for $\mathbf{x}_s = [-5, -5, -5, -5]$ due to the lack of sufficient gradients. At first glance, one could expect that this might be caused by the very low Reynolds numbers, but Fig. 14 indicates that this is not the case, and the problem also remains for the maximum investigated $Re = 5 \cdot 10^5$ (which might still be considered a low Reynolds number but usually is in a range where flow separation and boundary-layer effects are not the major problems). This problem of signal-to-noise ratio can partly be overcome by implementing a minimum angle change in the optimization routine.

2) For high-positive as well as high-negative local angles of attack, flow separation occurs on the vortex diffuser blades. This can also be noticed in Fig. 12. As forces for separated flow are unsteady, it is difficult to identify the gradients to calculate blade angles for the next iteration step.

3) Since the transient behavior of the force balance is very slow, the waiting and measuring times must be long. This increases the time needed for an optimization run and the total wind-tunnel time significantly.

The optimization process could be improved by using the inverse lift-to-drag ratio C_D/C_L as the target variable in the minimization problem. In this case, the problems with signal-to-noise ratio are expected to decrease, as certain changes in blade angles do not affect drag very much but do change lift. So minimization of C_D/C_L (equivalent to finding the maximum lift to drag ratio) would result in easier gradient detection.

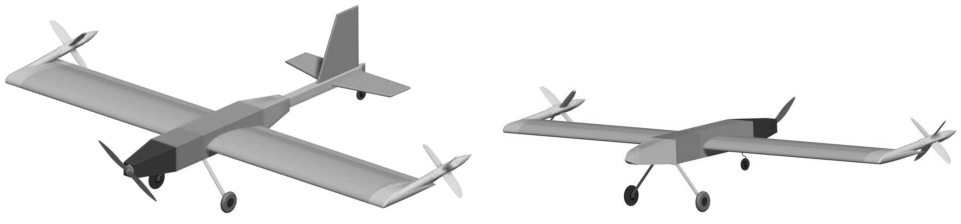

a) b)

Fig. 11 CAD outline of an experimental UAV in conventional configuration with a) additional vortex diffusers and b) and wing–body configuration without tail.

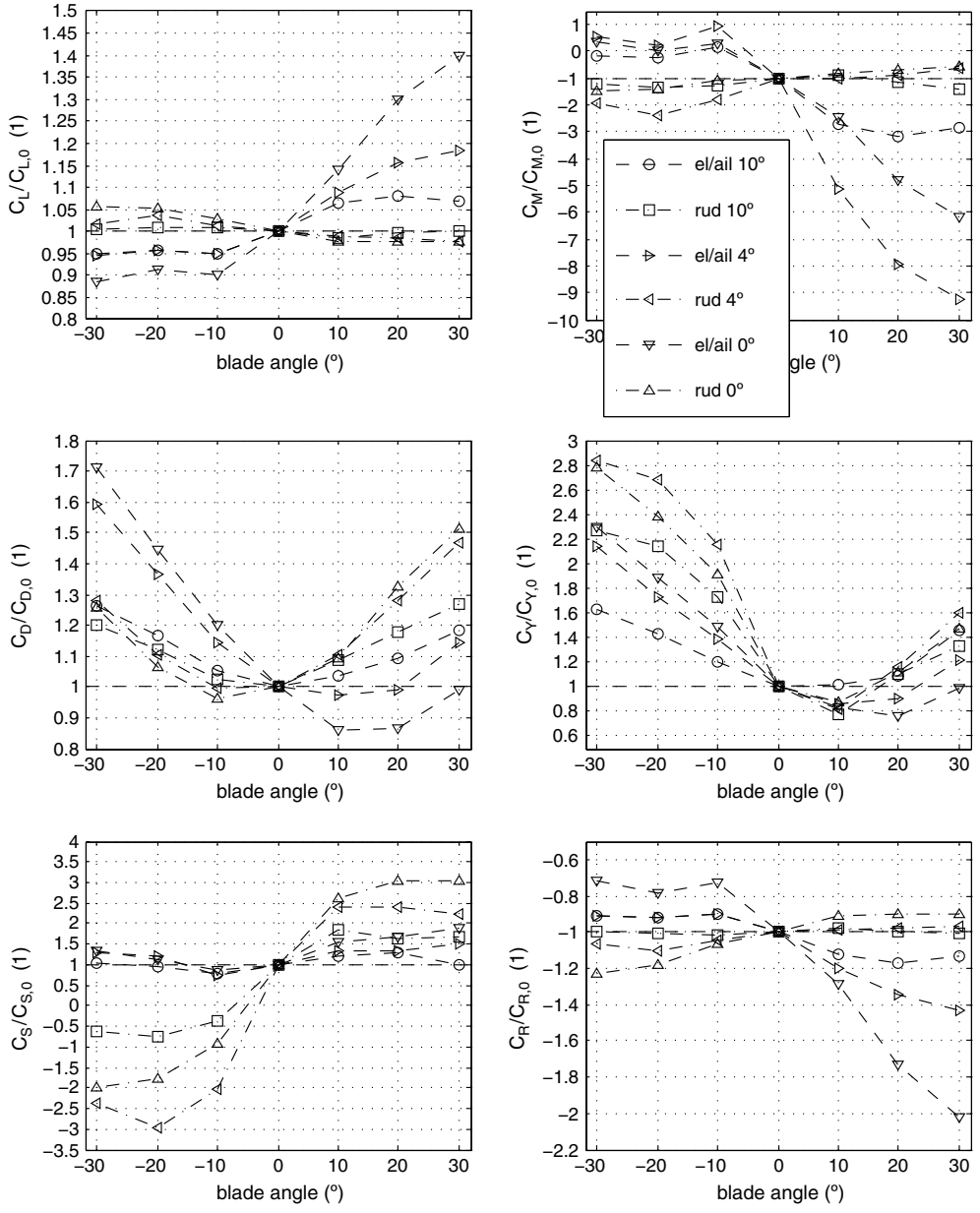

Fig. 12 Coefficients of forces and moments due to vortex diffuser acting as elevator/aileron and rudder for 10, 4, and 0° angles of attack of the main wing.

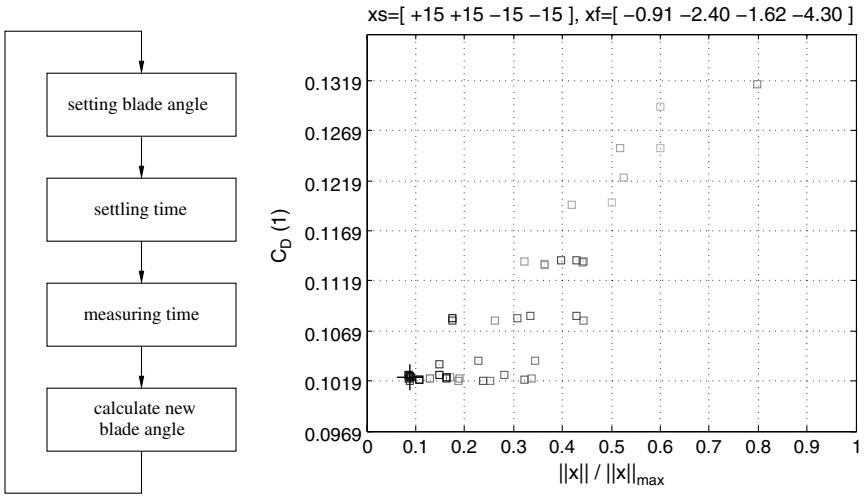

a) Optimization loop **b) Visualization of optimization progress**

Fig. 13 Optimization process.

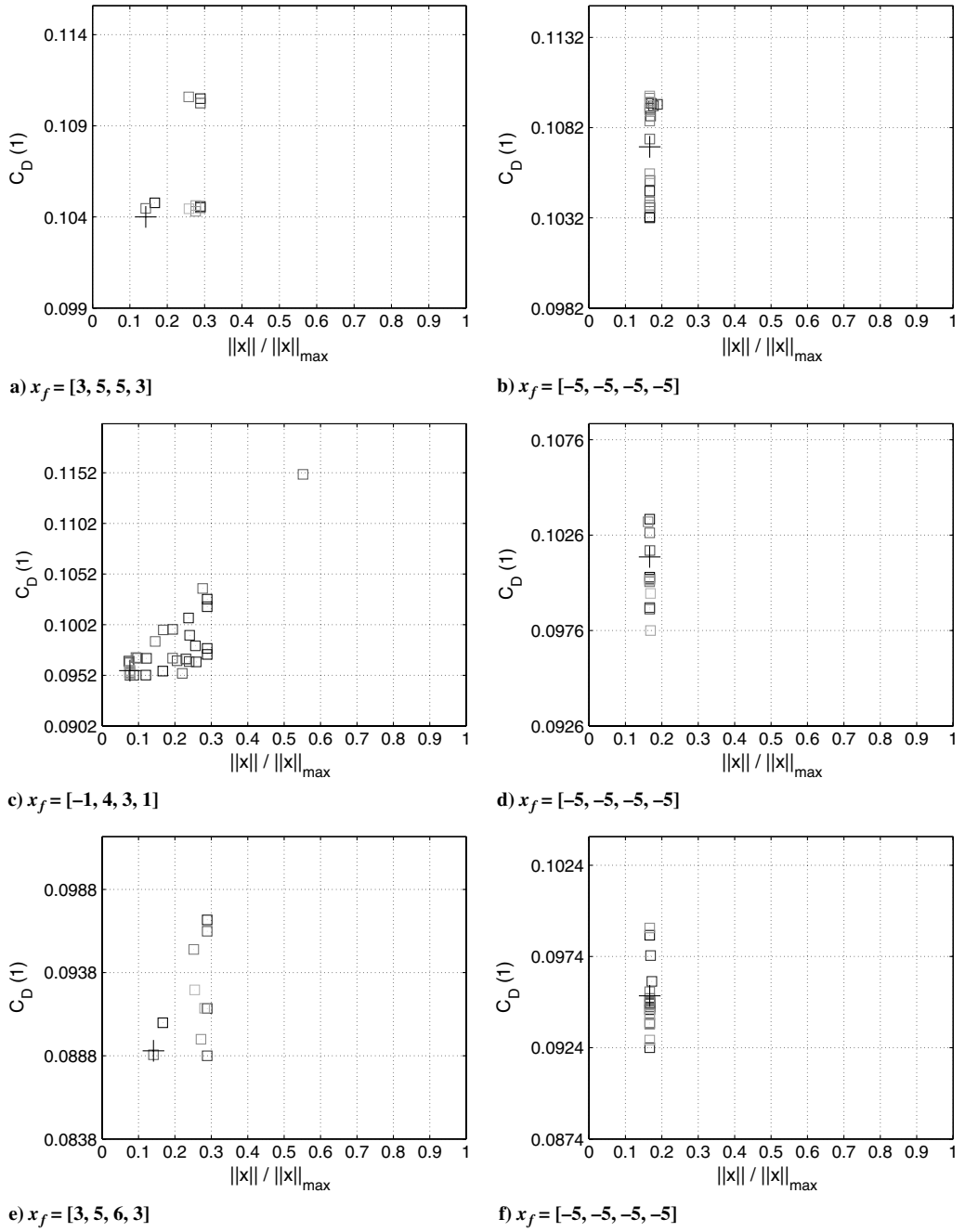

Fig. 14 Optimization results for start values of x_s = [5, 5, 5, 5] and x_s = [−5, −5, −5, −5] for the following Reynolds numbers: a and b) $Re = 1.6 \cdot 10^5$, c and d) $Re = 3.3 \cdot 10^5$, and e and f) $Re = 4.9 \cdot 10^5$.

IV. Conclusions

The paper demonstrated a design study for a vortex diffuser on a rectangular wing in high-lift/high-angle-of-attack configurations.

It was shown that by having sufficiently accurate information about the tip vortex immediately behind the trailing edge, the lifting-line theory was able to calculate thrust-producing vortex diffuser surfaces. Wind-tunnel tests were able to validate a significant drag reduction for high-lift/high-angle-of-attack configurations matching the numerically predicted values very well.

The significant difference between predicted and achieved lift and drag data in the second measurement session indicates that it was not possible to achieve the assumed symmetry of the vortex roll up in all wind-tunnel experiments. This also remains the main problem for the practical application of a vortex diffuser.

Improvements can be achieved by individual setting of the blade angles, leading to a minimization problem with four degrees of freedom. A viable approach for finding minimal drag in the wind-tunnel experiment is an in-the-loop optimization of vortex diffuser settings. Since differences in drag forces for small blade angle variations are close to the balance threshold, optimization results are limited by the resolution of the available experimental setup.

Wind-tunnel experiments also demonstrated that blade forces and moments show a feasible behavior for using the vortex diffuser as a steering device. By limiting the blade deflections to $\pm 10°$, a linearized control model could be used to describe flight mechanics of a vortex diffuser on a wing–body configuration without a rudder/elevator.

References

[1] Kroo, I., "Drag due to Lift: Concepts for Prediction and Reduction," *Annual Review of Fluid Mechanics*, Vol. 33, 2001, pp. 587–617. doi:10.1146/annurev.fluid.33.1.587

[2] Hackett, J., "Vortex Drag Reduction by Aftmounted Diffusing Vanes," International Councity of the Aeronautical Sciences, Munich, ICAS

Paper 80-13.4, 1980, pp. 542–553.
[3] Wimmer, P., "Experimentelle Untersuchung Aerodynamischer Strömungsvorgänge im Bereich Widerstandsmindernder Zusatzelemente Eines Tragflügels," Ph.D. Thesis, Johannes Kepler Univ. of Linz, Austria, 2005.
[4] Krieger, M., "Numerische Untersuchung der Umströmung Eines Tragflügels Sowie von Zusatzelementen zur Verringerung des Induzierten Widerstandes," Ph.D. Thesis, Johannes Kepler Univ. of Linz, Austria, 2009.
[5] Mehrle, A. H., "Extension of Multhopp's Quadrature Method to Cyclic Periodic Lifting Systems," *Acta Mechanica*, Vol. 202, Nos. 1–4, 2009, pp. 135–144.
doi:10.1007/s00707-008-0017-7
[6] Mehrle, A. H., "Über die Optimale Gestaltung von Widerstandsmindernden Zusatzelementen Eines Tragflügels," Ph.D. Thesis, Johannes Kepler Univ. of Linz, Austria, 2006.
[7] Schmitz, F. W., *Aerodynamik des Flugmodells*, Luftfahrtverlag Walter Zuerl, Wörthsee, Germany, 1942, pp. 148–150.
[8] Puttinger, S., "Experimentelle Untersuchungen zum Prinzip des Vortex Diffusers," Ph.D. Thesis, Johannes Kepler Univ. of Linz, Austria, 2009.
[9] Lyon, C. A., Broeren, A. P., Giguere, P., Gopalarathnam, A., and Selig, M., *Summary of Low-Speed Airfoil Data*, Vol. 3, SoarTech Publ., Virginia Beach, VA, 1997, pp. 405–406.
[10] Selig, M., Donovan, J., and Fraser, D., *Airfoils at Low Speeds*, SoarTech Publ., Virginia Beach, VA, 1989, pp. 390–391.